

## A NUMERICAL MODEL ON SALT MIGRATION IN A CLOSED UNSATURATED FINE SAND COLUMN WITH TEMPERATURE GRADIENTS

**Augustus C. Resurreccion**

Department of Engineering Sciences  
University of the Philippines, Diliman, Quezon City  
Philippines

### ABSTRACT

*Solute transport in the unsaturated zone in nonisothermal conditions has its important applications in the field of agriculture and groundwater quality modeling. In this research, the phenomena of simultaneous transport of moisture, heat and solute in the unsaturated porous media are formulated by three partial differential conservation equations. Numerical simulation and experimental study on salt migration is carried out in a closed unsaturated fine sand (Toyourra sand in Japan) column. Numerical discretization and solution are performed on the experimental domain with appropriate boundary conditions by iterative Picard technique Galerkin Finite Element Method. Results show that salt, in initial uniform water content and solute concentration, accumulates at the bottom due to heat source by salt precipitation and moisture convection. The characterization of the identified hydraulic parameters with temperature is also discussed.*

### I. Introduction

Several authors have studied the salt migration in the unsaturated zone. Most studies formulated mathematical models on simultaneous transport of water, heat and solute. Temperature gradients and presence of solute has a salient effect in the moisture transport. Thus Richard's equation together with convection-dispersion of solute transport must be modified. Nassar and Horton [1989 a, b] discussed the effect of temperature and solute content in the water flux in steady state conditions by computing liquid and vapor diffusivities due to water content, temperature and solute concentration gradients. The theoretical aspect based on Philip and de Vries mechanistic approach on simultaneous transport on unsaturated nonisothermal salty soil has been investigated by Nassar and Horton [1992a] using liquid water ( $\theta_l$ ) based formulation of the water transport equation and verified by Nassar, Horton and Globus [1992b] column experiments. Bear and Gilman [1995] studied the migration of salts near a hot boundary in the unsaturated zone and predicted the increase in salts near the heating source. Simunek and Suarez [1994] discussed the transport of reactive salts in isothermal conditions with upstream residual technique for convection-dispersion equation.

*Bear, Bensabat and Nir* [1991] discussed the different initial water content conditions that may lead to different water content distributions at steady state. When the initial water content is lower than a certain critical value, considerable drying occurs in the hot boundary. *Milly* [1982] formulated a matric potential ( $\psi_m$ ) based model of heat and moisture transport that takes into account the hysteresis effect and inhomogeneity of the porous media. Modifications are made in the model of *Milly* [1982] to include the non-reactive solute transport from *Nassar and Horton* [1992a]. *Yakirevich, et. al.* [1997] studied completely the transport of water, heat and reactive salt solution with adsorption and ion exchange and its effect in evaporation and solved the transport equations using finite difference method. The present study aims at modeling the migration of solutes of non-reactive salts in the unsaturated porous media with a proposed modified mathematical model.

The research is focused on how temperature and solute content affect water flow and as a consequence how much salt is transported. Assumption on non-reactive solute, neglecting adsorption and ion exchange, results to simplified conservation equations. No effect of solute concentration on unsaturated hydraulic conductivity and matric potential is further assumed. The resulting partial differential equations are discretized, and finite element formulation of the equations is employed to generate the numerical solution of salt migration under temperature gradients in the unsaturated porous media.

## II. Mathematical Model

The moisture transport equation is formulated by applying continuity equation on the Representative Elementary Volume (REV) and evaluating flux equations by separately analyzing liquid and vapor phases (*Milly* [1982]). The vapor flux is modified Fickian diffusion law and the liquid flux is from unsaturated Darcy's law. The moisture transport equation is

$$\left[ \left( 1 - \frac{\rho_v}{\rho_l} \right) \frac{\partial \theta_l}{\partial \psi_m} + \frac{\theta_a}{\rho_l} \frac{\partial \rho_v}{\partial \psi_m} \right] \frac{\partial \psi_m}{\partial t} + \left[ \left( 1 - \frac{\rho_v}{\rho_l} \right) \frac{\partial \theta_l}{\partial T} + \frac{\theta_a}{\rho_l} \frac{\partial \rho_v}{\partial T} \right] \frac{\partial T}{\partial t} + \left[ \left( 1 - \frac{\rho_v}{\rho_l} \right) \frac{\partial \theta_l}{\partial C} + \frac{\theta_a}{\rho_l} \frac{\partial \rho_v}{\partial C} \right] \frac{\partial C}{\partial t} = \frac{\partial}{\partial z} \left( D_{\psi_m} \frac{\partial \psi_m}{\partial z} + D_T \frac{\partial T}{\partial z} + D_C \frac{\partial C}{\partial z} + K \right) \quad (1)$$

The primary variables are matric potential ( $\psi_m$ ), temperature (T) and solute concentration (C).  $\theta_l$  is the liquid water content,  $\rho_l$  is the liquid water density,  $\theta_a$  is the air filled porosity,  $\rho_v$  is the absolute humidity and K is the unsaturated hydraulic conductivity. The coordinate z-axis is positive upwards. The diffusivities expressed into liquid and vapor components denoted by subscripts L and V respectively.  $D_{\psi_m} = D_{\psi_{mv}} + D_{\psi_{ml}}$  is the diffusivity due to matric potential gradient,  $D_T = D_{TV}$  is the diffusivity due to temperature gradient,  $D_C = D_{CV} + D_{CL}$  is diffusivity due to solute concentration gradient. The diffusivities are given by the following equations

$$\begin{aligned}
D_{\psi_m} &= \frac{1}{\rho_l} D_{\text{atm}} \Omega \theta_a \frac{\partial \rho_v}{\partial \psi_m} + K \\
D_r &= \frac{1}{\rho_l} D_{\text{atm}} f' \xi \frac{\partial \rho_v}{\partial T} \\
D_c &= \frac{1}{\rho_l} D_{\text{atm}} \Omega \theta_a \frac{\partial \rho_v}{\partial C} - K \frac{\sigma \phi R_v T_k}{\rho_l g}
\end{aligned} \tag{2}$$

$D_{\text{atm}} = 2.29 \times 10^{-5} (T_k/273)^{1.75}$  is the molecular diffusivity of water vapor in air in  $\text{m}^2/\text{s}$ ,  $\Omega = \theta_a^{2/3}$  is the tortuosity factor of the air-filled pores,  $\phi = 0.93$  is osmotic coefficient for NaCl,  $\sigma$  is the osmotic efficiency,  $R_v$  is the gas constant for water vapor,  $g$  is gravitational acceleration and  $T_k$  is the absolute temperature.

The thermal enhancement factor ( $f'$ ) is

$$\begin{aligned}
f' &= n & \theta_l \leq \theta_k \\
f' &= \theta_a + \frac{\theta_a}{n - \theta_k} \theta_l & \theta_l > \theta_k
\end{aligned} \tag{3}$$

in which  $\theta_k$  is the liquid water content at which flow becomes negligible, that is the order of vapor diffusivity ( $D_{\psi_m}$ ) magnitude is greater than that of unsaturated hydraulic conductivity  $K$ , and  $n$  is the porosity of the medium. The parameter  $\xi$  is the ratio of the average temperature gradient in the air,  $(\nabla T)_a$ , with the overall average (macroscopic) temperature gradient  $(\nabla T)$ ,

$$\xi = \frac{(\nabla T)_a}{\nabla T} \tag{4}$$

The thermodynamic relationship of water vapor density ( $\rho_v$ ) with matric potential ( $\psi_m$ ), osmotic potential ( $\psi_o$ ) and absolute temperature ( $T_k$ ) is given by *Philip and de Vries* [1957] on the assumption of thermodynamic equilibrium between liquid and vapor phases.

$$\rho_v = \rho_o \exp\left(\frac{(\psi_m + \psi_o)g}{R_v T_k}\right) \tag{5}$$

The saturation vapor density,  $\rho_o$ , is the density at saturation vapor pressure at which a change of phase can occur at a constant temperature. The saturated vapor density can be obtained  $\rho_o = 10^{-3}(19.84 - 4975.9/T_k)$   $\text{kg}/\text{m}^3$  (*Kimball et. al.* [1976], *Nassar and Horton* [1989b]).

The unsaturated hydraulic conductivity relationship with volumetric liquid water content is also corrected by temperature and is expressed by  $K = K_s k_r k_T$  where  $K_s$  is the saturated hydraulic conductivity,  $k_r$  is the relative hydraulic conductivity at reference temperature and  $k_T = \mu_T / \mu_{T_0}$  is the temperature factor given by the ratio of the dynamic viscosity at reference temperature  $T_0$  with the dynamic viscosity at temperature  $T$ . The solute effect on unsaturated hydraulic conductivity is neglected. The unsaturated hydraulic conductivity,  $K(\theta_l)$ , and soil water retention curve,  $\psi_m(\theta_l)$ , used in the numerical model are from the *van Genuchten* [1980] model.

$$\frac{K(\theta_1)}{K_s} = \theta_c^{\frac{1}{2}} \left\{ 1 - \left[ 1 - \theta_c^{\frac{1}{m}} \right]^m \right\}^2 \quad (6)$$

$$\theta_c = \frac{\theta_1 - \theta_r}{\theta_s - \theta_r} = \left[ \frac{1}{1 + (\alpha \psi_m)^n} \right]^m \quad (7)$$

$\theta_e$  is the effective water content defined by the equation (7).  $\theta_r$  and  $\theta_s$  are the residual water content and the saturated water content respectively.  $\alpha$ ,  $m$  and  $n$  are identified coefficients from the experimental data.

According to Milly [1982], the thermal vapor diffusivity is sensitive to temperature and insensitive to the liquid water content except at dry condition.

The heat flow is formulated from *de Vries* [1958] and solute effect on heat flow is incorporated and is expressed by

$$\begin{aligned} & [(L_0 + c_p(T - T_0))\theta_a \frac{\partial \rho_v}{\partial \psi_m} + ((c_1 \rho_1 - c_p \rho_v)(T - T_0) - L_0 \rho_v - \rho_1 W) \frac{\partial \theta_1}{\partial \psi_m}] \frac{\partial \psi_m}{\partial t} + \\ & [C_v + (L_0 + c_p(T - T_0))\theta_a \frac{\partial \rho_v}{\partial T} + ((c_1 \rho_1 - c_p \rho_v)(T - T_0) - L_0 \rho_v - \rho_1 W) \frac{\partial \theta_1}{\partial T}] \frac{\partial T}{\partial t} + \\ & [(L_0 + c_p(T - T_0))\theta_a \frac{\partial \rho_v}{\partial C}] \frac{\partial C}{\partial t} = \frac{\partial}{\partial z} \left( \lambda \frac{\partial T}{\partial z} + \rho_1 L (D_{v_{mv}} \frac{\partial \psi_m}{\partial z} + D_{cv} \frac{\partial C}{\partial z}) - c_1 (T - T_0) q_m \right) \end{aligned} \quad (8)$$

$L$  is the latent heat of vaporization,  $L_0$  is the latent heat at reference temperature  $T_0$ ,  $W$  is the heat of wetting,  $c_1$  is specific heat of water,  $c_p$  is specific heat of vapor at constant pressure,  $\lambda$  is the soil effective thermal conductivity and  $q_m$  is the moisture flux.

The volumetric heat capacity of the porous medium is defined by  $C_v$

$$C_v = \sum_{i=1}^5 C_i \theta_i \quad (9)$$

where  $\theta_i$  and  $C_i$  are the volumetric fraction and volumetric heat capacity of the  $i^{th}$  soil constituent (*de Vries* [1958]).

The effective thermal conductivity ( $\lambda$ ) of the porous media is a function of liquid water content, matric potential and temperature, and is given as a weighted average,

$$\lambda = \left( \sum_{i=1}^5 k_i \theta_i \lambda_i \right) \left( \sum_{i=1}^5 k_i \theta_i \right)^{-1} \quad (10)$$

where  $k_i$  is the ratio of the average temperature gradient in the  $i^{th}$  constituent to the average temperature gradient of the bulk medium given as

$$k_i = \frac{2}{3} \left[ 1 + \left( \frac{\lambda_i}{\lambda_1} - 1 \right) g_i \right]^{-1} + \frac{1}{3} \left[ 1 + \left( \frac{\lambda_i}{\lambda_1} - 1 \right) (1 - 2g_i) \right]^{-1} \quad (11)$$

where the liquid phase is considered continuous and  $g_i$  is the ‘‘shape factor’’ of the  $i^{th}$  constituent. No value is given to  $g_1$  since the coefficient is zero. The value of  $g_2$  is considered a function of water content as follows (*Kimball et. al.* [1976], *Milly* [1984]).

$$g_2 = 0.013 + \left[ \frac{0.022}{\theta_w(pF = 4.2)} + \frac{0.298}{n} \right] \theta_l \quad \text{if } \theta_l < \theta_w (\text{at } pF = 4.2)$$

$$g_2 = 0.035 + \frac{0.298}{n} \theta_l \quad \text{if } \theta_l > \theta_w (\text{at } pF = 4.2) \quad (12)$$

The effective thermal conductivity of the air-filled pores, enhanced by vapor distillation is (*de Vries* [1958])

$$\lambda_2 = \lambda_a + D_{\text{atm}} L \left. \frac{\partial \rho_v}{\partial T} \right|_{\psi_m} \quad (13)$$

$\lambda_a$  is the thermal conductivity of dry air.

Finally, the solute transport is given by

$$\frac{\partial(\theta_1 C)}{\partial t} = -\nabla \cdot (Cq_l - \theta_l D_{\text{sh}} \nabla C - D_{T_m} \nabla T) \quad (14)$$

which is the conventional convection dispersion equation with the effect of temperature on molecular diffusion taken into consideration.  $D_{\text{sh}}$  is hydrodynamic dispersion,  $D_{T_m}$  is the enhancement of molecular diffusion due to temperature gradient and  $q_l$  is the volumetric liquid flux.

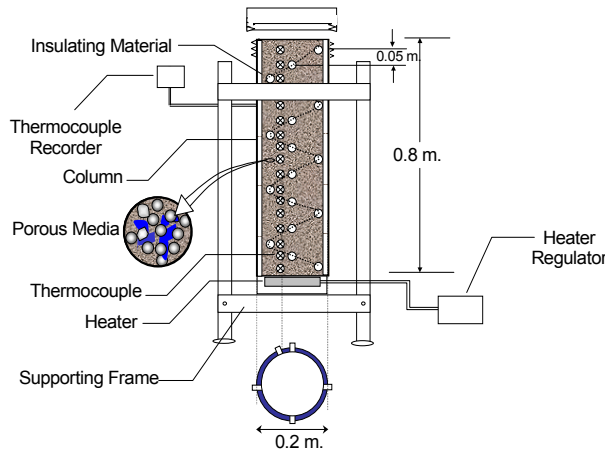


**Figure 1.** Schematic diagram of experimental apparatus

### III. Experimental Study

The experiments on simultaneous water, heat and solute transport are done on a closed soil column in controlled laboratory environment. The experimental set-up mainly consists of a fine sand column of 80-cm height and 20-cm diameter, thermocouple sensors, and a heater (Figure 1). Fine sand (Toyourra sand in Japan), used as the porous medium, has soil properties of porosity, 0.445, and saturated hydraulic conductivity,  $2 \times 10^{-4}$  m/s. The fine sand is cleaned to remove organic matter, washed for several times and soaked overnight before performing the experiment until the similar electrical

conductivity value before and after washing is reached. A sodium chloride salt solution is prepared to obtain specified initial water content with salt concentration for each case. The salt solution is mixed with fine sand thoroughly. The soil is packed inside the steel column and mounted on a heater to generate temperature difference at the ends of the column. The bottom end is at 50°C while the other end at 22°C constant ambient temperature in a regulated room. Thermocouples gauge the local temperature installed at 5-cm intervals along the soil column. At steady state (after three days), the soil sample is cut into 5-cm sections. Water content is gravimetrically computed, and salt concentrations are measured at each section by electric conductivity meter. Two supporting experiments (replicates) are also prepared to check the precision of the results.

#### IV. Numerical Solution

##### 4.1 Finite Element Formulation

A numerical simulation is carried out, and the results are compared with the experimental output. The SPLaSHWaTr (*Scanlon and Milly* [1994]) using Galerkin finite element method coded in Fortran is modified for the inclusion of solute transport computation. The governing equations for the simultaneous transport of water, heat and solute are described by the equations (1), (8) and (14). The form of the each transport equation can be written as

$$s_{w_1} \frac{\partial \psi_m}{\partial t} + s_{w_2} \frac{\partial T}{\partial t} + s_{w_3} \frac{\partial C}{\partial t} + \frac{\partial}{\partial z} (s_{w_4} \frac{\partial \psi_m}{\partial z} + s_{w_5} \frac{\partial T}{\partial z} + s_{w_6} \frac{\partial C}{\partial z} + s_{w_7}) = 0 \quad (15)$$

where the parameters  $s_{w_1}$  to  $s_{w_7}$  are defined implicitly by *equation* (15) and each transport equation. The solution is interpolated by using linear basis function  $N_j^e$  over the entire domain (Figure 2) by the trial functions

$$\hat{\psi}_m = \sum_j^n \psi_{m_j}(t) N_j^e \quad \hat{T} = \sum_j^n T_j(t) N_j^e \quad \hat{C} = \sum_j^n C_j(t) N_j^e \quad (16)$$

where  $j$  is the node index,  $n$  is the number of nodes,  $e$  references the element. The basis functions  $N_j^e$  are non-zero only on the element  $e$ ; with a value of unity at the node  $j$  linearly decreasing to zero at the other end node. Method of weighted residual (Galerkin) is applied, and using integration by parts, the finite element formulation results to

$$\begin{aligned} & \sum_{e=1}^{n-1} \int_e \left( s_{w_1} \frac{\partial \hat{\psi}_m}{\partial t} + s_{w_2} \frac{\partial \hat{T}}{\partial t} + s_{w_3} \frac{\partial \hat{C}}{\partial t} \right) N_j^e dz + \\ & \sum_{e=1}^{n-1} \int_e \left( s_{w_4} \frac{\partial \hat{\psi}_m}{\partial z} + s_{w_5} \frac{\partial \hat{T}}{\partial z} + s_{w_6} \frac{\partial \hat{C}}{\partial z} + s_{w_7} \right) \frac{dN_j^e}{dz} dz = \\ & -\delta_{i1} \left( \frac{\hat{q}_m}{\rho_1} \right) \Big|_{z=0} + \delta_{in} \left( \frac{\hat{q}_m}{\rho_1} \right) \Big|_{z=z_0} \end{aligned} \quad (17)$$

where  $\delta_{ij}$  is the kronecker delta. Substitution of the trial functions into the equation (17) yields a set of nonlinear algebraic equations.

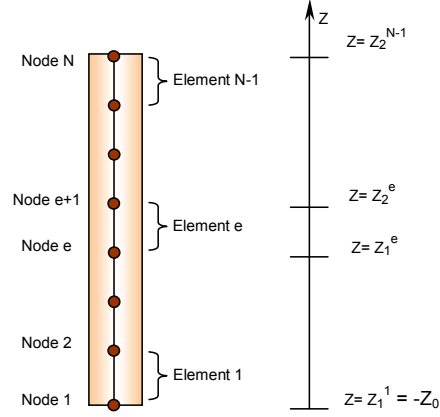


**Figure 2.** Discretization of the domain and coordinate system for the Finite Element Model

The finite element formulation in matrix form (indicial notation) is

$$\sum_{j=1}^n \left( a_{ij} \frac{\partial \psi_{m_j}}{\partial t} + b_{ij} \frac{\partial T_j}{\partial t} + c_{ij} \frac{\partial C_j}{\partial t} + d_{ij} \psi_{m_j} + e_{ij} T_j + f_{ij} C_j \right) + g_i = 0 \quad i=1, \dots, n \quad (18)$$

where the coefficients of the finite element formulation is given

$$\begin{aligned} a_{ij} &= \sum_e \int_{z_e} s_{w_1} N_i^e N_j^e dz & b_{ij} &= \sum_e \int_{z_e} s_{w_2} N_i^e N_j^e dz \\ c_{ij} &= \sum_e \int_{z_e} s_{w_3} N_i^e N_j^e dz & d_{ij} &= \sum_e \int_{z_e} s_{w_4} \frac{dN_i^e}{dz} \frac{dN_j^e}{dz} dz \\ e_{ij} &= \sum_e \int_{z_e} s_{w_5} \frac{dN_i^e}{dz} \frac{dN_j^e}{dz} dz & f_{ij} &= \sum_e \int_{z_e} s_{w_6} \frac{dN_i^e}{dz} \frac{dN_j^e}{dz} dz \\ g_i &= \sum_e \int_{z_e} s_{w_7} \frac{dN_i^e}{dz} dz + \delta_{i1} \left( \frac{\hat{q}_m}{\rho_1} \right) \Big|_{z=0} - \delta_{in} \left( \frac{\hat{q}_m}{\rho_1} \right) \Big|_{z=z_0} \end{aligned} \quad (19)$$

The parameters  $s_{w1}$  to  $s_{w7}$  are assumed to vary continuously only inside the elements, and discontinuity is only restricted at nodal points. The integrals may be approximated by assuming that the parameters  $s_{w1}$  to  $s_{w7}$  vary linearly inside the element (*Milly* [1982])

$$s_{wj} = \sum_{l=1}^n s_{wjl} \cup_e N_l^e \quad j = 1, 2, \dots, 7 \quad (20)$$

Temporal derivatives are estimated by finite difference using fully implicit backward difference scheme. At the old time level  $k$ , the nodal values of  $\psi_{mj}^k$  (primary variables) are known and that over the time increment  $\Delta t$  defined by the old and the current time levels,  $k$  and  $k+1$ , the nodal values vary linearly. It follows that the nodal values at time level  $k+\phi$  are computed by

$$\Psi_{m_j}^{k+\varphi} = \varphi \Psi_{m_j}^{k+1} + (1-\varphi) \Psi_{m_j}^k \quad (21)$$

where  $\varphi$  is a time weighing factor.

In this study, fully implicit scheme is used for temporal analysis. This scheme is obtained when  $\varphi$  has a value of one. The fully implicit scheme is unconditionally stable. Thus, time acceleration factor can be introduced

Whenever the solution is consistent, time acceleration can be utilized when the difference between the maximal changes in the primary variables and the specified targets is less than a tolerance error. The tentative increase/decrease factor for the change in time step  $\Delta t$  can be calculated on basis of maximum changes of state. This factor is limited by not allowing an excessively large increase in  $\Delta t$ . However, if a large decrease in  $\Delta t$  is required, this is indicative of an excessive change of state during the most recent time step. This time step is repeated using the smaller  $\Delta t$ . In this study, space discretization the specific target for the change in primary variables is 10 cm, 1<sup>0</sup>C, 0.002 and 0.0005 g/cm<sup>3</sup> for matric potential, temperature, volumetric liquid water content and solute concentration respectively.

Due to strong nonlinearity of the coefficients, Picard iteration technique is used, and Thomas algorithm for resulting linear systems is utilized per iteration (*Huyankorn and Pinder* [1983]). Similar formulation can be obtained for heat transport. The solute transport equation as expressed in the conservative form is reformulated by applying the continuity equation resulting to

$$\theta_1 \frac{\partial(C)}{\partial t} = \frac{\partial}{\partial z} (D_{sh} \theta_1 \frac{\partial C}{\partial z}) - q_1 \frac{\partial(C)}{\partial z} \quad (23)$$

For this type of advection-dispersion equation, it is recommended to adopt the method of upstream weighted residual technique to eliminate the effect of numerical dispersion in a convection dominated solute flow.

#### 4.2 Method of Weighted Upstream Residual

It is well known that the advective-dispersive transport equation is more difficult to solve numerically than flow equation. The problem is particularly severe when advection dominates over dispersion. In this situation, the Galerkin Finite Element Method exhibits numerical oscillations (overshoot and undershoot) near the concentration front. These oscillations can be eliminated numerical oscillations by upstream residual technique. This application is made in such a manner that the spatial and the temporal derivatives in the equation are both weighted using asymmetric weighing functions. These are obtained by adding quadratic functions to the linear basis functions.

### 4.3 Boundary Conditions and Computational Flowchart

The boundary conditions for the closed system, which is the conducted experiment, are of no flux for water flow and solute flow whereas the temperatures at the boundaries are specified constants. The computational flowchart is shown in Figure 3. The solution to the transport equation follows the finite element procedure of generating the coefficient matrix, finite difference approximation of the temporal derivatives, assembling the global matrix, imposing the boundary conditions and solving the resulting tridiagonal matrix by Thomas algorithm.

The water transport equation is first solved holding the previous values of temperature and solute concentration. The matric potential is hence computed from the water transport equation which other primary variables are held to be known. The heat transport equation is solved next with the recent computed value of matric potential but still using the previous value of the solute concentration variable. Finally, solute transport is solved with recent computed values of matric potential and temperature.

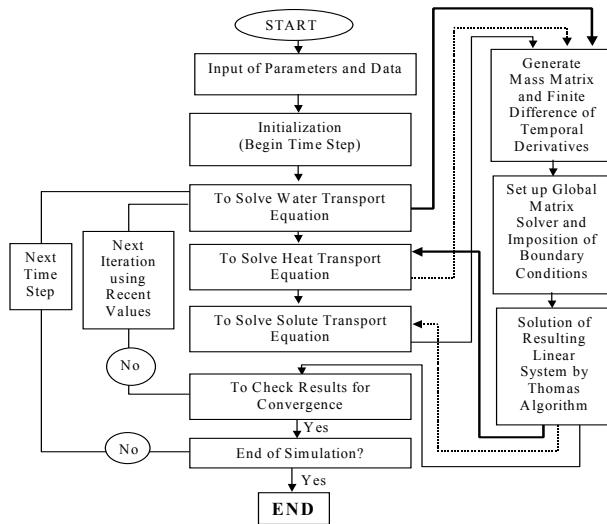


**Figure 3.** Computational flowchart and algorithm

## V. Results

### 5.1 Comparison of experimental data with numerical simulated results for 10% initial water content, 3% solute concentration and nonisothermal

Figures 4, 5 and 6 illustrate the variation of the water content, temperature, solute concentration profiles along fine sand column for the experimental case of 10% initial water content, 3% initial solute concentration and nonisothermal conditions (28 C<sup>0</sup> temperature gradient). Three replicates are conducted and the comparison shows good agreement among the measured

values. The differences in measured values could be attributed to average sampling of soil at 5-cm sections and slight differences in the initial conditions. The results, however, are generally acceptable.

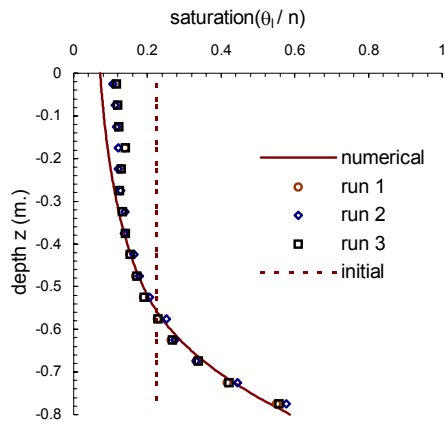
Figure 4 illustrates the degree of saturation profile showing increasing water content to the bottom of the closed column. Computation of the total water contained in the soil column by comparing the area of the initial water content with the area made by the water content profile for the mass balance reveals 6.6% loss of total water in the column. The loss is from the vapor unaccounted in gravimetric water measurements in exposing the sample to ambient conditions while sampling. Figure 5 shows a nonlinear distribution of temperature from cold end increasing to the heated end. This is attributed to the variable moisture content since thermal conductivity and volumetric heat capacity are also dependent on soil water content as explained in the calculation of soil thermal properties by *Philip and de Vries* [1957] model. Temperature gradients, consequently, affects moisture flow since vapor transport is an important aspect of moisture flow phenomena while the vapor phase is often neglected in the isothermal models using the traditional Richards' equation. Though it is much smaller than the effect of liquid diffusivity (matric potential gradient) in liquid flow, the effect becomes appreciable for very dry soil layer with low water content. The deviation of the experimental measured temperatures with the computed values from numerical simulation is attributed from the heat loss to the periphery of the experiment.

The solute concentration profile is shown in Figure 6. There is much scattering or variation among the measured values, however the trend is similar. The factors affecting the deviation of the values are the sensitivity of the electric conductivity meter for salt concentration measurement, the average sampling of the soil column into 5-cm sections, and the inexact replication of the initial conditions for the preparation of the soil sample. However, comparison of the average of the three replicates with the simulated results shows slight difference. Solute concentration balance gives 1.33% loss by comparing the area to the left and right of the solute initial concentration.

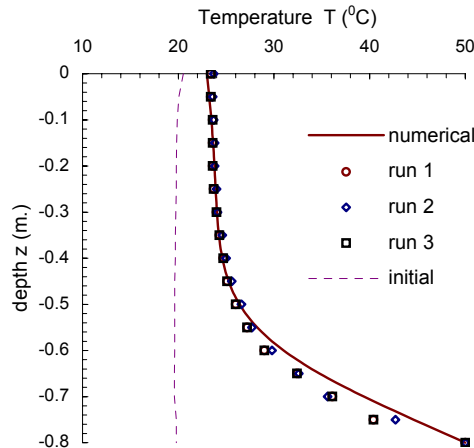
## 5.2 *Physical mechanism of transport*

Figure 7 shows the schematic diagram of the phenomena of liquid and vapor flow in the soil sample. Vapor and liquid phases are analyzed separately, however these transport of vapor and liquid phases are occurring simultaneously. Initially, the water content variation in the soil column is uniform. Gravity effect dominates and liquid water percolates to the bottom. The soil water content profile shows that the water content increases to the bottom though it is a heated end. Temperature gradients inducing phase change enhance vapor flow, where from the almost saturated heated end, *evaporation* occurs. The vapor traverses the air-filled pores (*vapor flux*), and condenses in the upper region of lower temperature. Temperature gradients can cause the water to move in the vapor phase from a hot site to condense at the cold site. Flow is reestablished whenever sufficient matric potential

gradient and osmotic potential gradient is achieved. After vapor condensation, a total pressure head gradient can drive water from the cold end to the hot site. Solute is carried by flowing liquid (*liquid flux*) and transported to the bottom of the column (*advective salt flux*). This contributes basically to the conveyance of solute toward the lower end. Due to the solute gradient, *diffusive salt flux* occurs in the direction away from the heat source. The solute effect on water flow is caused by the osmotic potential that is created from the differences in solute concentration. This effect, however, is only comparable with the effect of temperature on liquid flow. The heat flux for the system is, of course, towards the cold end. The main feature of thermally induced water movement in the unsaturated zone is that it involves also evaporation, condensation and movement of water vapor. These affect the efficiency of heat transfer and cause soil moisture redistribution (Bear, Bensebat and Nir [1991]).



**Figure 4.** Degree of saturation profile of the column with initial water content of  $0.1 \text{ m}^3/\text{m}^3$ ,  $28^\circ\text{C}$  temperature gradient at ends and 3% solute concentration by weight



**Figure 5.** Temperature profile of the column with initial water content of  $0.1 \text{ m}^3/\text{m}^3$ ,  $28^\circ\text{C}$  temperature gradient at ends and 3% solute concentration by weight

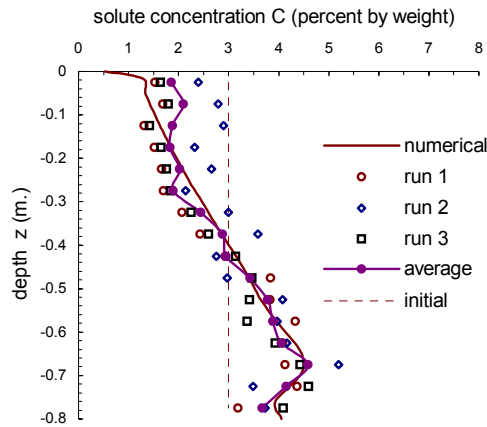


**Figure 6.** Salt concentration profile of the column with initial water content of  $0.1 \text{ m}^3/\text{m}^3$ ,  $28^\circ\text{C}$  temperature gradient at ends and 3% solute concentration by weight

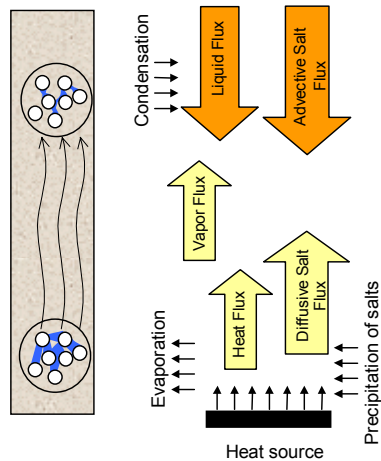


**Figure 7.** Schematic diagram of the physical mechanism of flow water content analysis (adopted from the figure of Bear and Gilman [1995])

### 5.3 Solute concentration analysis

The transport mechanism for solute is through convection by liquid flow and diffusion due to the solute concentration gradient. *Nassar and Horton* [1997] also found a reduction in water transfer toward the cold end of the salty soil material. Water vapor pressure is a function of temperature and

solute concentration. Figure 8 and 9 show the variation of solute concentration for different initial water content in isothermal and nonisothermal conditions. Solute is carried to the bottom through convection in relatively wet initial conditions (25% initial water content). Figure 8 shows the numerical output of solute concentration profile from different initial water content in isothermal cases with 3% initial salt concentration. The profiles show almost similar trend of increasing solute content to the bottom of the column. The isothermal conditions did not change the water content profile in a relatively dry initial conditions that minimal convection and diffusion of salt to the bottom of the column takes place. Simulated results with initial water content of 20% and 25% show high concentration at the bottom.

Comparing with Figure 9, which is the nonisothermal case, the same trend can be observed though there is a slight increase in value for relatively wet conditions (20% and 25%). Except for the dry case of 5% initial water content, a considerable increase in the amount of solute can be found near the heat source. The convected solute to the bottom becomes precipitate due to phase change of water from liquid to vapor phase, which makes the salt solution not capable of dissolving salts, and hence precipitation occurs.

Figure 10 and 11 show the outcome of the numerical simulated solute concentration profiles for 5% and 10% initial water content. It can be inferred from the figure that solute concentration is conserved in the sand column based on the area to the left and right of the initial solute concentration. A vertical hump can be observed for wet initial conditions (Figure 11). The increase in solute can be attributed to the increased water flow due to evaporation and condensation cycle in the mechanism of flow.

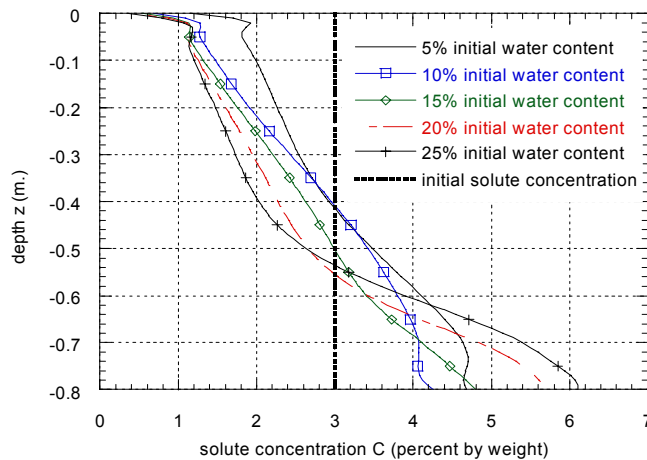


**Figure 8.** Numerical results of solute concentration profiles for isothermal cases of 5 to 25% initial volumetric water content. The initial solute concentration is 3% by weight.

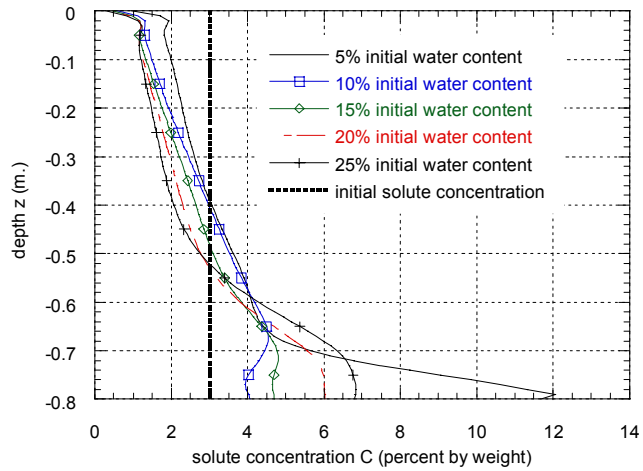


**Figure 9.** Numerical results of solute concentration profiles for nonisothermal cases of 5 to 25% initial volumetric water content. The initial solute concentration is 3% by weight.

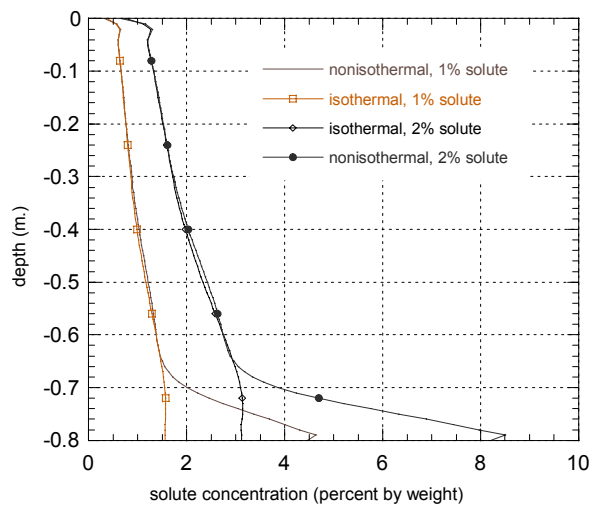


**Figure 10.** Solute concentration profiles with 5% initial volumetric water content (numerical simulation results)

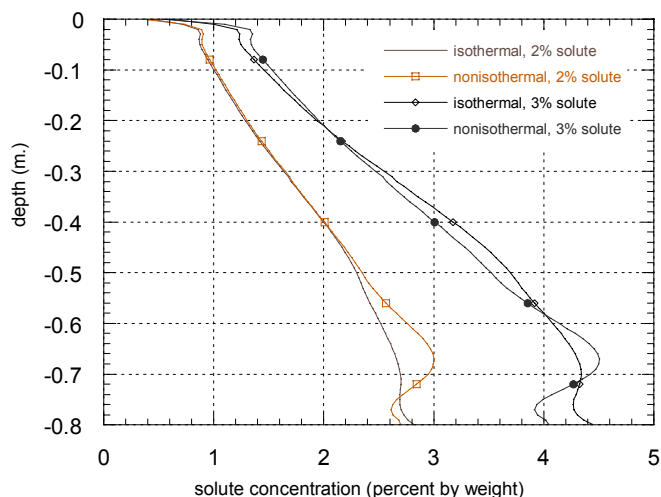


**Figure 11.** Solute concentration profiles with 10% initial volumetric water content (numerical results)

#### 5.4 Characterization of identified parameters

Figure 12 shows the change in matric potential and thermal conductivity due to the effect of temperature. For constant volumetric water content, temperature decreases the value of matric potential. It is evident from the figure the sudden decrease in matric potential at very low water contents (less than 0.01) and near saturation (greater than 0.4). This is indicative of a rapid release of water from the pores or drainage. Between these extreme regions, the soil moisture retention curve has a gentle slope in the semi-log scale. The thermal conductivity increases with increasing water content and temperature. At low water content, the value of thermal conductivity is greatly affected by the temperature. This is due to the increase in diffusion coefficient in high air-filled space (that is low water content) with high temperature. *Nassar and Horton [1997]* concluded that the model of *de Vries* can be used for accurately predicting the apparent thermal conductivity for low solute concentration, an intermediate water content and temperature range of 20<sup>0</sup>C to 50<sup>0</sup>C. The thermal conductivity of the porous medium in unsaturated zone is sensitive to temperature. Figure 13 to 15 illustrate the effect of temperature and volumetric water content on liquid and vapor diffusivities for temperatures 20<sup>0</sup>C-50<sup>0</sup>C and concentration of 3 percent by weight. The unsaturated hydraulic conductivity increases with water content. The change due to temperature is less than with the increase due to water content. For vapor diffusivities, temperature change can bring great differences in value in very low water content. For a temperature change of 30<sup>0</sup>C, the vapor diffusivity is magnified five times. For high temperature, the transport of latent heat by vapor distillation is positively affected by temperature and negatively affected by water content.

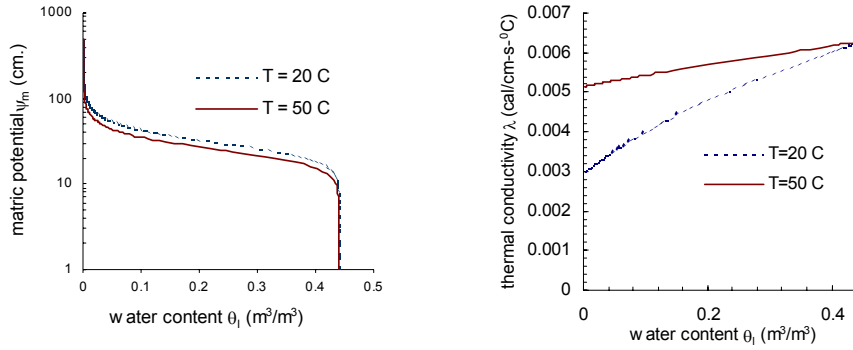


**Figure 12.** Variation of matric potential and thermal conductivity with temperature and liquid water content

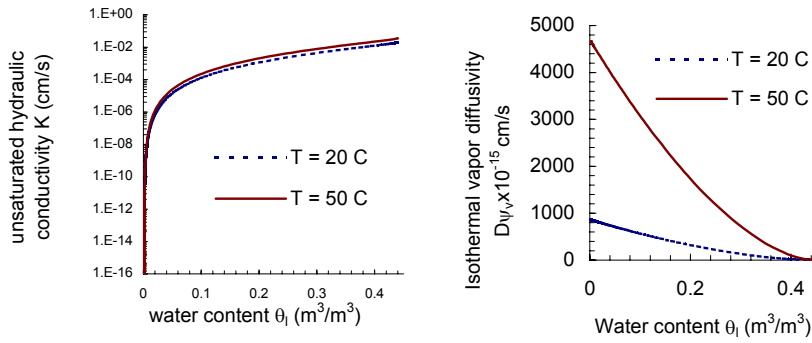


**Figure 13.** Variation of unsaturated hydraulic conductivity and isothermal vapor diffusivity with temperature and liquid water content

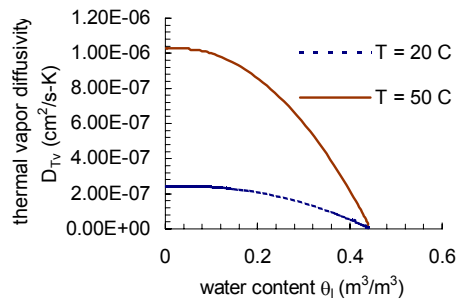


**Figure 14.** Variation of thermal vapor diffusivity with temperature and liquid water content

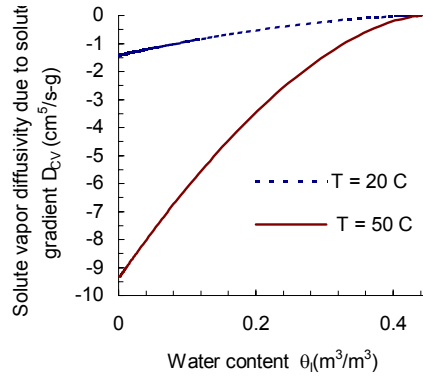


**Figure 15.** Variation of vapor diffusivity due to solute concentration gradient with temperature and liquid water content

## VI. Conclusions

The theoretical model consists of three partial differential equations describing water, heat and solute transport in unsaturated porous media. Galerkin Finite Element Method solves these equations with upstream residual technique applied to the convection dispersion equation. Results show that temperature and solute content plays a major role in the movement of water. The following points can be observed from this research. Water generally flows to the bottom of the column due to the enhancement of vapor flux by temperature. The vapor condenses at the colder region establishing a sufficient matric potential gradient for liquid flux to occur. Water content increases near the heat source in relatively wet nonisothermal condition. However for the case of relatively dry initial water content, existence of dry layer can be observed near the heat source. The temperature gradients bring great changes in thermal conductivity due to high thermal diffusion coefficient, which increases vapor distillation. Although the temperature effect in the liquid region is not significant, the temperature effect on vapor phase has appreciable impact in dry or barren areas where evaporation is a major consideration for moisture budget in soil atmosphere interaction. The heat source acts as a magnet for the solute. Within the boundary of the heat source, significant drying occurs where liquid water evaporates into vapor. The amount of salt convected to the bottom is already considerable that the solubility of salt decreases rapidly. The salt solution becomes “saturated” and precipitation occurs. Water changing into vapor phase in the hot domain leaves solute residuals behind, therefore as a consequence accumulation of salts occurs.

## References

1. Bear, J. “Dynamics of Fluids in Porous Materials”, American Elsevier, (1972).
2. Bear, J., Bensabat J. and Nir A., “Heat and mass transfer in unsaturated porous media at a hot boundary, I. One-dimensional analytical model”, *Transport in Porous Media* 6, 281-298, (1991).

3. Bear, J., Gilman A. "Migration of salts in the unsaturated zone caused by heating", *Transport in Porous Media* 19, 139-156
4. Bear, J. and A. Verruijt. "Modeling Groundwater Flow and Pollution", Kluwer Academic Publ., (1987).
5. de Vries, D.A. "Simultaneous transfer of heat and moisture in porous media". *Trans. Am. Geophys. Union* 39:909-916, (1958).
6. Helmig, R., "Multiphase Flow and Transport Processes in the Subsurface", Springer-Verlag, (1997).
7. Huyakorn, W., and Pinder, G, "Computational Methods in Surface and Subsurface Hydrology", (1983).
8. Kay, B.D. and P.H. Groenevelt, "On the interaction of water and heat on frozen and unfrozen soils 1. Basic Theory; the vapor phase", *Soil. Sci. Soc. Am. Proc.* 38(3), 395-400, (1974).
9. Kimball, B.A., R.D. Jackson, R.J. Reginato, F.S. Nakayama, and S.B. Isdo, "Comparison of field measured and calculated soil heat fluxes", *Soil. Sci. Soc. Am. J.* 40, 18-28, (1976).
10. Milly, P.C.D., "Moisture and heat transport in hysteretic, inhomogenous porous media: A matric head-based formulation and numerical mode", *Water Resour. Res.*, 18(3), 489-498, (1982).
11. Milly, P.C.D., "A simulation analysis of thermal effects on evaporation from soil", *Water Resour. Res.*, 20(3), 1087-1098,(1984).
12. Nassar, I. N., and R. Horton, "Water transport in unsaturated non-isothermal salty soil I, Experimental results", *Soil. Sci. Soc. Am. J.* 53(5), 1323-1329, (1989a).
13. Nassar, I. N., and R. Horton, "Water transport in unsaturated non-isothermal salty soil, II, Theoretical development", *Soil. Sci. Soc. Am. J.* 53(5), 1330-1337, (1989a).
14. Nassar, I. N., and R. Horton, "Simultaneous transfer of heat, water, and solute in porous media, I, Theoretical development", *Soil. Sci. Soc. Am. J.* 56(5), 1350-1356, (1992).
15. Nassar, I. N., and R. Horton., and A.M. Globus, "Simultaneous transfer of heat, water, and solute in porous media, I, Experiment and analysis", *Soil. Sci. Soc. Am. J.* 56(5), 1357-1365, (1992).
16. Nassar, I. N., and R. Horton, "Heat, water, and solute transfer in unsaturated porous media, I, Theory development and transport coefficient evaluation", *Transport in Porous Media* 27, 17-38, (1997).
17. Philip, J.R. and D. A. de Vries, "Moisture movement in porous materials under temperature gradients". *Trans. Am. Geophys. Union* 38:222-232, (1957).
18. Robinson, R.A. and R. H. Stokes, "Electrolyte Solutions", Butterworths, London
19. Scanlon B.R. and P.C.D.Milly, "Water and heat fluxes in desert soils", *Water Resour. Res.*, 30(3), 721-733, (1994).
20. Simunek, J., and D.L. Suarez, "Two dimensional transport model for variably saturated porous media with major ion chemistry", *Water Resour. Res.*, 30(4), 1115-1133, (1994).
21. Van Genuchten, M.Th., "A closed form equation for predicting the hydraulic conductivity of unsaturated soils", *Soil. Sci. Soc. Am. J.* 44, 892-896, (1980).
22. Warrick, A.W., J. W. Biggar and D. R. Nielsen, "Simultaneous solute and water transport for an unsaturated soil", *Water Resour. Res.*, 7(5), 1216-1225, (1971).
23. Yakirevich, A., Berliner, P., Sorek, S., "A model for numerical simulating of evaporation from bare saline soil", *Water Resour. Res.*, 33(5), 1021-1033, (1997).